RSC Advances

ROYAL SOCIETY OF CHEMISTRY

www.rsc.org/advances

Cite this: DOI: 10.1039/c0xx00000x

www.rsc.org/xxxxxx

ARTICLE TYPE

The contribution of friction to electrorheological properties of chrysanthemum-like particles suspension

Xufeng Dong,*[a] Ning Ma,[b] Hui Yang,[a] Baoguo Han,[b] and Min Qi*[a]

Received (in XXX, XXX) Xth XXXXXXXXX 20XX, Accepted Xth XXXXXXXXX 20XX

DOI: 10.1039/b000000x

Several studies have proved that significant electrorheological (ER) effect can be obtained by using the particles with hierarchic structures as the dispersing phase. The inter-particle friction and fluid friction caused by the rough surface of the particles plays an important role for their enhanced ER effect. However, the detailed contribution of friction to ER properties remains unclear. We prepare two different ER fluids with chrysanthemum-like particles and spherical particles, respectively. We carry out low shear velocity oscillation test to separate the friction-induced shear stress from the electrostatic attraction-induced shear stress. The chrysanthemum-like particles-based ER suspension presents much better ER performance than the ER fluid with spherical particles. The larger friction force caused by the rougher surface of chrysanthemum-like particles is a major reason for the improvement. The contribution of friction to ER effect depends on electric field strength. The contribution has a maximum value at a critical electric field.

1 Introduction[a]

As a kind of smart materials, electrorheological (ER) fluids present drastic changes in their rheological properties by applying an electric field.[1-3] ER fluids consist of highly polarizable micron- or nano-sized particles dispersed in insulation oils. The particles are aggregated to form chain-like or column-like structures under an electric field, which leads the ER fluids transit from a liquid state to a solid-like state, and the yield stress increases with increasing electric field. Once the electric field is withdrawn, the original disordered state is recovered, indicating the change of the rheological properties is reversible.[4-6] Compared with magnetorheological fluids, which have been widely used in various fields, ER fluids exhibit rapider response time, simpler mechanics and lower energy consumption. Therefore, ER fluids have attracted considerable attention, and have been regarded as potential smart materials for application in microfluidic chips, microactuators, dampers, clutches, brakes, orthotic devices, etc.[7-10]

Since the ER effect was discovered by Winslow in 1949, several mechanisms have been proposed to explain and predict the ER behavior of conventional ER fluids, the yield stress of which was less than 10 kPa at 5 kV/mm.[11-14] Those models included water bridge model, double electrode layer model, electric polarization model, conduction model, and dielectric mismatch model. In 2003, a giant electrorheological (GER) fluid composed by urea-coated barium titanyl oxalate (BTRU) nanoparticles suspended in silicone oil was discovered.[15] The yield stress of the GER fluid was ~130 kPa at 5 kV/mm. Since then, considerable efforts have been made to prepare different particles with high ER performance. Those particles included core/shell particles, polar molecule modified particles, nanocomposites, semiconductive polymers, etc.[16-24] The yield stresses of those new ER fluids were two orders magnitude larger than that of the conventional ones, which cannot be explained by the conventional mechanisms. Therefore, several new models have been proposed, such as saturation polarization model, polar-molecule-dominated model, and saturated orientational polarization of polar molecules model. [25-27]

In all of those models, the particles are assumed as smooth sphere, and the yield stress is dominated by the attractive force among the particles. Recently, some particles with rough surface were used to prepare ER fluids with high ER performance. Wang et al used kaolinite/TiO_2 nanopapillar particles and bionic cactus-like titanium oxide microspheres to prepare new ER fluids.[25-27] They claimed that the ER properties can be greatly improved by using rough surface particles, and the friction between adjacent particles is responsible for the improvement. Besides, Jaeger's experimental results indicated that the yield stress of the ER fluids can be enhanced by applying larger normal stress, which indirectly proved that the friction force influences the ER properties.[30] All of those studies indicated the friction including inter-particle friction and fluid friction plays an important role on the yield stress of ER fluids. Tian et al has studied the effect of friction through shear thinning and shear thickening characteristics of ER fluids.[31-33] Li et al has proposed a model to

[a] *School of Materials Science and Engineering, Dalian University of Technology, Dalian 116024, China. Email: dongxf@dlut.edu.cn*

[b] *School of Civil Engineering, Dalian University of Technology, Dalian 116024, China.*

study the effect of friction on magnetorheolgoical fluids, and Zhuang used similar model investigate the frictional stress of starch ER fluids and STO ER fluids.[34] The inter-particle friction coefficient they obtained was a constant, because they assumed that the particles only form chain-like structures under an electric field. However, as observed in various studies, column-like structures would be formed at high field levels, in which case the friction among the adjacent particles would be more complex. Besides, the particles they used were smooth sphere, and the effect of the inter-particle friction was only indirectly studied by exerting normal stress. Therefore, more complex model should be established to analysis the contribution of friction to properties of ER fluids, and rough surface particles should be used to study the effect of friction directly. In this paper, the friction was theoretically analyzed based on column-like structure. Besides, chrysanthemum-like particles with rough surface were used to prepare an ER fluid, and its rheological properties were tested to study the contribution of friction.

2. Modelling

Figure 1 shows the evolution of aggregation state of particles with increasing electric field strength, which also can be observed in SI.1 (movie). Initially, the particles are randomly dispersed in the media without order. At a small external field, the particles aggregate to form chain-like structures, and low yield stress is observed. As the electric field increases, the chains capture more free particles to form column-like structures, in which case the yield stress is greatly enhanced. By calculating the Coulomb potential energy, the column structures arrange themselves with body centered tetragonal (BCT). [25]

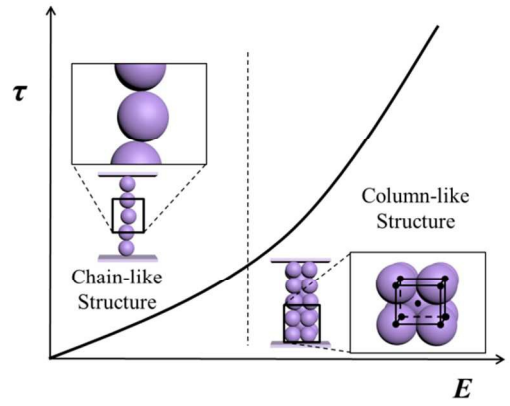

Figure 1. Evolution of aggregation state of particles with increasing electric field strength

As the particles aggregation state varies with electric field, the contact state among the adjacent particles changes. For chain-like structures, as shown in Fig.1, every particle contacts with two neighboring particles along the field direction, which is the simplest situation. In that case, the inter-particle friction force is proportional to the normal force and friction factor. As the electric field increases, the single chain-like structures transfer to BCT structures, in which case every particle contacts with 8 neighboring particles, as shown in Fig.1. Obviously, the contact state of the adjacent particles is much more complex in column-like structures than that in chain-like structures. The dependence of the inter-particle friction force on the normal force and friction factor is nonlinear. Considered the complexity, it is difficult to get the direct expression of the inter-particle friction force. Besides, it is also difficult to separate the friction force with the attractive force under quasi-static loading.

Under oscillatory tests, ER fluids present viscoelastic behavior, which has been observed in various studies. As viscoelastic materials, their shear stress τ depends on the complex modulus G^* and shear strain γ. Under small strain amplitude, ER fluids are considered as linear viscoelastic materials. Therefore, their complex modulus G^* is dominated by the electric field and the angular frequency. Since the shear strain γ changes with time, the shear stress τ can be demonstrated by the following equation

$$\tau(t) = G^*(E,\omega)\gamma(t) \quad (1)$$

where G^* can be expressed as

$$G^* = G' + iG'' \quad (2)$$

where G' and G'' are defined as the storage modulus and the loss modulus, respectively. The storage modulus G' is dominated by the attractive force among the particles, which is related to the elastic energy. By contrast, the loss modulus G'' is related to the dissipated energy during the oscillation. Under oscillatory measurements, the ER fluids could dissipate the energy through the hydrodynamic force caused by the particles' motion in media, the fluid friction, or the inter-particle friction. Nevertheless, at low shear velocity, or at low shear strain amplitude with a constant oscillatory frequency, the energy dissipated by the hydrodynamic force is insignificant compared with that dissipated by the inter-particle friction and fluid friction. Therefore, the dissipated energy can be considered dominated by fiction.

According to Equ.1 and Equ.2, the relationship between the shear stress amplitude τ_0 and the shear strain amplitude γ_0 is

$$\begin{aligned}\tau_0 &= \left|G^*(E,\omega)\right|\gamma_0 \\ &= \sqrt{G'(E,\omega)^2 + G''(E,\omega)^2}\,\gamma_0\end{aligned} \quad (3)$$

The shear elastic stress amplitude τ_{e0} and the shear friction stress amplitude τ_{f0} can be obtained by the following equations,

$$\tau_{e0} = G'(E,\omega)\gamma_0 \quad (4)$$

$$\tau_{f0} \approx G''(E,\omega)\gamma_0 \quad (5)$$

The contribution of friction on the shear stress is defined by the following equation

$$C_f = \frac{\tau_{f0}^2}{\tau_0^2} \quad (6)$$

It can be expected that, as the aggregation state changes from randomly dispersed particles to column-like structures with increasing electric field, both the electric induced stress and friction induced stress will increase. The questions needed to be answered are which one plays the dominated role, and whether the proportion of the two parts changes with changing electric field.

3. Experimental

3.1 Synthesis of chrysanthemum-like and spherical particles

All chemicals were of analytical grade and used without further purification. The starting materials included titanium butoxide (TBOT, $Ti(C_4H_9O)_4$) , glycerol, and anhydrous ethanol.

Chrysanthemum-like particles were synthesized by a solvothermal method. Firstly, 2 g TBOT and 10 g glycerol were dissolved in 23.7 g anhydrous ethanol to form homogeneous solution A and solution B, respectively. Secondly, the solution A and the solution B were mixed uniformly by electromagnetic stirring at 25℃. After refluxing for 10 min, the resulting mixture was transferred into an 80 ml Teflon-lined autoclave, which was sealed tight and maintained at 180 ℃ for 24 h. After being cooled to room temperature naturally, the precipitates were filtered and washed with ethanol, followed by drying at 80℃ in a vacuum oven.

Similar procedure was used to prepare smooth spherical particles. The starting solution composed by 2 g TBOT dissolved in 47.4 g ethanol, and no glycerol was added into the solution. The homogeneous solution was transferred into an 80 ml Teflon-lined autoclave and heated at 180℃. After 24 h, the autoclave was cooled to room temperature. The resulting product was filtered and washed with ethanol, followed by drying at 80℃ in a vacuum oven.

3.2 Preparation of ER fluids

Dimethyl silicone oils with kinematic viscosity of 50 cSt were used as the carrier liquid to prepare ER fluids. To avoid the influence of moisture, silicone oils were dried at 120 ℃ for 2 h before the preparation. Besides, the particles were milled for 5 hours in a mortar and dried in a vacuum oven at 80 ℃ for 2 hours to remove physical adsorbed water. The concentration of the two ER fluids was 20% by effective volume.

3.3 Characteristics

The structures of the particles were identified by means of X-ray diffraction (XRD) with an Empyrean X-ray diffractometer (PANalytical, Netherland) with Cu Kα radiation (λ=1.5418 Å) at a scan rate of 0.04 s^{-1}. Their morphologies were investigated by a field emission scanning electron microscopy (FESEM, NOVA NANO 450SEM, America). Transmission electron microscopy (TEM) observation was obtained on a Tecnai G220 S-Twin microscope (FEI, USA). Fourier transform infrared spectroscopy (FTIR, EQUINOX55, Germany) was employed to determine the basic nature of samples with a KBr disk method. The dielectric relaxation spectra of the two kinds of particles were measured using a WK6500B dielectric spectrometer (Wayne Kerr, UK). The frequency of the AC electric fields ranged from 20 Hz to 15 MHz.

The electrorheological properties of the ER fluids at different DC electric field were measured by a Physica MCR 301 rheometer (Anton paar, Austria) with the PP15-E parallel plates measuring system. The diameter of the plates was 15 mm and the gap between the two plates was 1 mm. The dependence of the yield stress on electric field strength was measured in the approach of quasi-static mode, in which the shear rate was kept constant at 0.2 s-1 while the electric field linearly increased from 0 kV/mm to 5 kV/mm. To find the linear viscoelastic region of the two ER fluids, strain amplitude sweep (0.01%~10%) measurements were carried out at a constant frequency 1 Hz and various electric fields (1kV/mm, 2kV/mm, 3kV/mm, and 4kV/mm). Finally, at fixed frequency (1 Hz) and fixed strain amplitude (0.1%), electric field sweeps were carried out. All the samples were measured at 25℃. The shear stress amplitude, storage modulus and loss modulus can be obtained in those dynamic measurements.

4. Results and discussion

4.1 Morphological and structural characteristics

The SEM images of the spherical particles and chrysanthemum-like particles are shown in Fig.2a and Fig.2b, respectively. The obtained spherical particles present uniform diameters (~1.5 μm) and smooth surface, as shown in Fig.2a. In contrast, dense thorn-like petals are observed on the surface of the chrysanthemum-like particles (Fig.2b). Since the adjacent chrysanthemum-like particles entangle with each other by their petals, it is difficult to observe the detailed structures. Figure 2c is the TEM image of the chrysanthemum-like particles. It reveals that the chrysanthemum-like particles are composed of several dozen thorn-like nanopetals. The average diameter of the particles is ~1.5 μm. The nanopetals of the chrysanthemum-like particles present radial distribution from the center of the particles. According to Reference 35, the formation process of the chrysanthemum-like particles can be illustrated by Fig.3. Initially, TBOT react with ethanol to produce spherical particles. With the increase of the reaction time, the spherical particles react with glycerol to form nanothorns and nanowires. As the reaction proceeded, those nanothorns and nanowires interweave into petals. After 24 h, chrysanthemum-like particles with nanopetals are obtained. Since the nanopetals are derived from the spherical particles rather than coating or grafting on their surface, they are expected to have better stability. After the milling process for preparing ER fluids, the nanopetals still exist. Due to their rough surface and comparable particle size with the spherical particles, the chrysanthemum-like particles are good candidates to study the effect of friction on properties of ER suspensions.

Figure 4 shows the XRD results of the spherical particles and the chrysanthemum-like particles. No sharp peaks are observed in their XRD patterns, indicating both of them are amorphous materials. For chrysanthemum-like particles, the wide peaks at 10° and 20° indicates the formation of titanium glycerolate (TiGly) phase. It corresponds well with the formation process illuminated by Fig.3.

The FTIR spectra of glycerol, the spherical particles and the chrysanthemum-like particles are shown in Fig.5. For the spherical particles, the characteristic *v* (O-H) vibration is observable at 3415 cm^{-1}, as shown in curve b. Curve c is the spectrum of chrysanthemum-like particles, in which the characteristic of *v* (O-H), *v* (C-H), and *v* (C-O) vibrations of glycerol are observed at 3419, 2920 and 1216 cm^{-1}, respectively. Compared with the spectrum of glycerol, the bonds of *v* (O-H) vibration of the chrysanthemum-like particles is narrow, which is due to the crystalline nature of the material. Besides, the bond at 1049 cm^{-1} corresponding to C–O stretching vibration of glycerol shifts to higher wavenumbers in the spectrum of chrysanthemum-like particles. It indicates the C-O bond coordinates to the titanium ions.

Figure 6 is the dielectric relaxation spectra of the spherical particles and the chrysanthemum-like particles. The dielectric

constant of the two kinds of particles decreases as the electric field frequency increases. At the same electric field, the spherical particles have higher dielectric constant than the chrysanthemum-like particles. The dielectric constant is related to polarizability.[6] An ER fluid with significant ER performance requires that the particles have a large $\Delta\varepsilon$' where

$$\Delta\varepsilon' = \varepsilon'_{100\text{Hz}} - \varepsilon'_{100\text{kHz}} \quad (8)$$

Compared with the chrysanthemum-like particles, the spherical particles have larger $\Delta\varepsilon$', indicating stronger interfacial polarization.

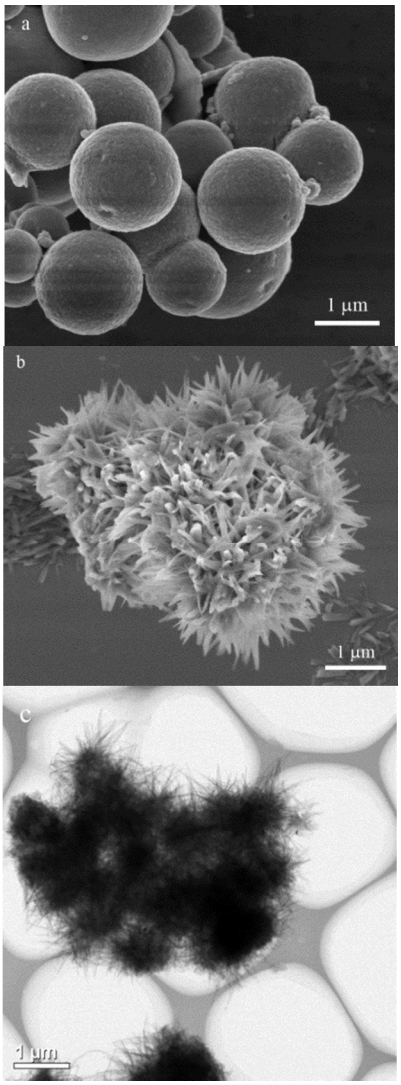

Figure 2. SEM images of (a) spherical particles and (b) chrysanthemum-like particles and (c) TEM images of chrysanthemum-like particles

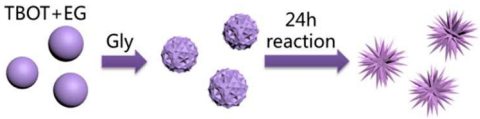

Figure 3. Schematic illustration of the chrysanthemum-like particles formation

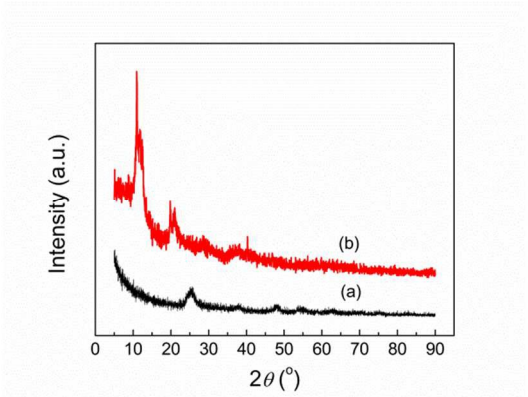

Figure 4. XRD patterns of (a) spherical particles and (b) chrysanthemum-like particles

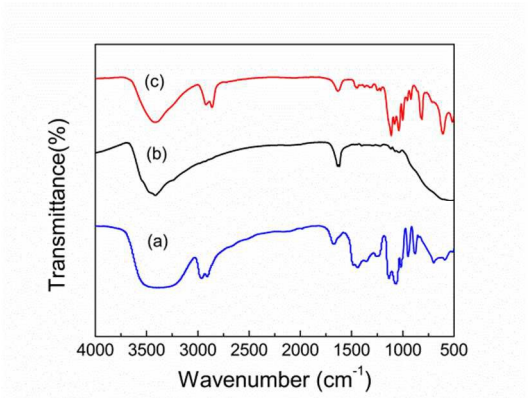

Figure 5. Infrared spectra of (a) glycerol, (b) spherical particles and (c) chrysanthemum-like particles

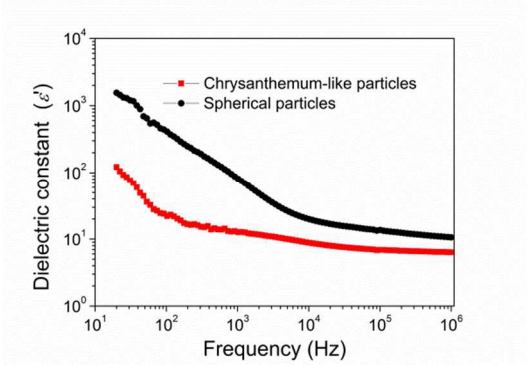

Figure 6 Dielectric constant as a function of the electric field frequency for spherical particles and chrysanthemum-like particles

4.2 Yield stress under quasi-static test

Figure 7 shows the relationships between the yield stress of the two kinds of ER fluids and electric field. As the electric field strength increases, both the chrysanthemum-like particles suspension and spherical particles suspension present increasing yield stress, indicating ER effect. At low field level, the change of yield stress with changing electric field is gently, while at high field level, their yield stress dramatically promotes. At the same field, the chrysanthemum-like particles-based ER fluid (C-ERF) presents higher yield stress than the spherical particles-based one (S-MRF). The difference between their yield stresses becomes increasingly significant as the electric field strength increases. At

5 kV/mm, the yield stress of the chrysanthemum-like particles-based ER fluid is about twice as large as the material prepared with the spherical particles.

There are four possible reasons for the better ER activity of the chrysanthemum-like particles-based ER fluid. First, due to their different chemical structures, the chrysanthemum-like particles may have higher dielectric constant than the spherical particles, which would enhance the attractive force between adjacent particles. However, as proved by the dielectric spectra of the two kinds of particles (Fig.6), the spherical particles have large $\Delta\varepsilon$'. It indicates the better ER properties of the chrysanthemum-like particles are caused by some other reasons. The second possible reason is that glycerol may provide polar groups on the surface of the chrysanthemum-like particles, which could improve the attractive force between adjacent particles, as stated by the polar molecule dominated mechanisms. The third possible reason is that the chrysanthemum-like particles may have higher conductivity than the spherical particles. However, the experimental results provide little support for this reason; the spherical particles present higher conductivity than the chrysanthemum-like particles over a broad frequency range from 20 Hz to 1MHz. (SI.2) The last possible reason is that the chrysanthemum-like particles have rougher surface, which could enhance the inter-particle friction force and promote the stress required to destroy the ordered structures. Proverbially, the inter-particle friction force is dominated by the normal stress and the friction factor between the adjacent particles. Figure 8 shows the dependence of the normal stress on electric field. As it is shown, the normal stress presents increasing tendency as the electric field increases, which is gentle at low field level and becomes dramatic at high field level. Nevertheless, under the same electric field, S-ERF presents higher normal stress than the C-ERF. The possible reason is that the smooth spherical particles could form more perfect BCT structures with higher density than the structures formed by the chrysanthemum-like particles. The stereo micrographs (Fig.9) of the two ER fluids at 2 kV/mm confirm the conjecture. Although the rough surface of the chrysanthemum-like particles prevents them to form perfect BCT structures, it improves the friction factors between adjacent particles.

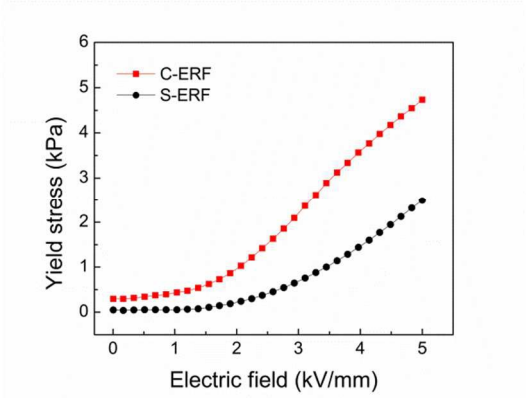

Figure 7. Yield stress of chrysanthemum-like particles ER fluid (C-ERF) and spherical particles ER fluid (S-MRF) as a function of electric field strength

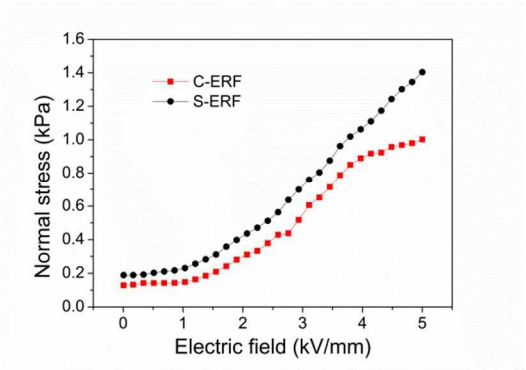

Figure 8. Dependence of the normal stress of chrysanthemum-like particles ER fluid (C-ERF) and spherical particles ER fluid (S-MRF) on electric field

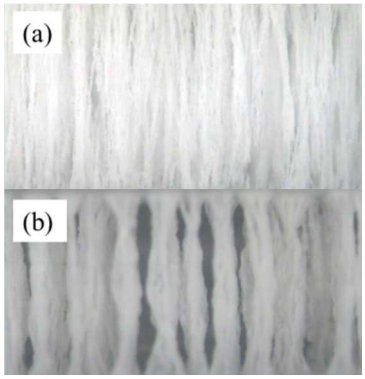

Figure 9. Stereo micrographs of chrysanthemum-like particles ER fluid (C-ERF) and spherical particles ER fluid (S-MRF) at 2 kV/mm

4.3 Friction under oscillatory test

Figure 10 shows the dependence of the dynamic shear moduli, including storage modulus *G'* and loss modulus *G"*, on strain amplitude at a constant frequency of 1 Hz. Under applying external electric field, the storage modulus of the two ER fluids keeps unchanged at low strain amplitude and then decreases with increasing strain when it reaches a critical value, while the loss modulus initially slightly increases and then decreases. Below the critical strain amplitude, the ER fluids are considered in their linear viscoelastic (LVE) regions. When the strain amplitude exceeds the critical value, the chains or columns formed by the magnetized particles becomes unstable, and the ER fluids are in nonlinear viscoelastic regions.

As indicated by Fig.10, both the C-ERF and the S-ERF are considered in LVE regions at fixed 0.1% strain amplitude, approximately. The dependence of the dynamic moduli of the two ER fluids on electric field at 0.1% stain amplitude and 1 Hz is shown in Fig.11. As the electric field increases, both the storage modulus and the loss modulus of the two ER fluids increase. Such an increasing tendency is gently at low field levels, and becomes dramatically at high field levels. Under the same field, the storage modulus of the two fluids is higher than their loss modulus, indicating the field induced attractive force plays a dominated role. Besides, both the storage modulus and the loss modulus of the chrysanthemum-like particles-based ER fluid are larger than those of the spherical particles-based ER fluid. It

indicates the C-ERF has larger field induced attractive force and larger friction force than the S-ERF.

The dependence of the stress amplitude, including total shear stress amplitude, the field induced stress amplitude, and the friction stress, on electric field is shown in Fig.12. As the electric field increases, the stress amplitudes of the two ER fluids rise. Under the same electric field, the field-induced stress amplitudes of the two ER fluids approach their total shear stress amplitudes, and are much higher than their friction-induced stress amplitudes. It further indicates that the field-induced stress is the dominate stress that influence the shear stress of the ER fluids. It also can be observed from Fig.12 is that the friction stress of the chrysanthemum-like particles-based ER fluid is much higher than that of the spherical particles-based ER fluid at the same electric field. The difference can be attributed to their different surface roughness.

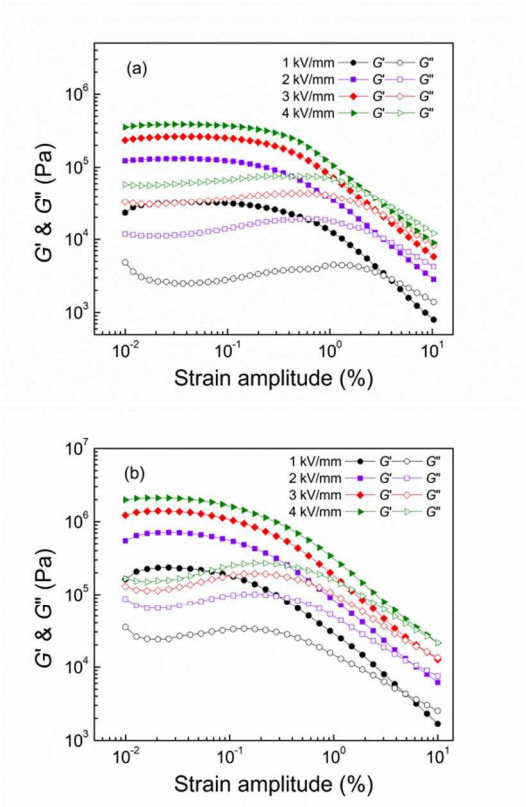

Figure 10. Dependence of the dynamic shear moduli (storage modulus *G*' and loss modulus *G*") of (a) chrysanthemum-like particles ER fluid (C-ERF) and spherical particles ER fluid (S-MRF) on strain amplitude at a constant frequency of 1 Hz

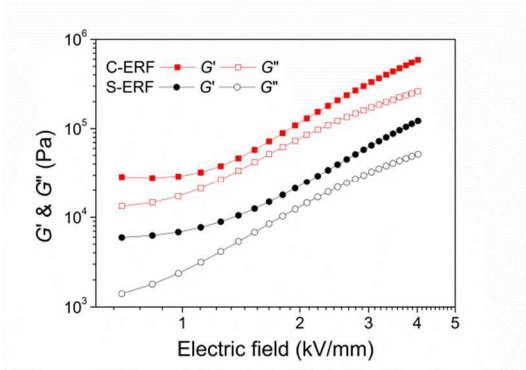

Figure 11. Dependence of the dynamic moduli (storage modulus G' and loss modulus G") of chrysanthemum-like particles ER fluid (C-ERF) and spherical particles ER fluid (S-MRF) on electric field at 0.1% stain amplitude and 1 Hz

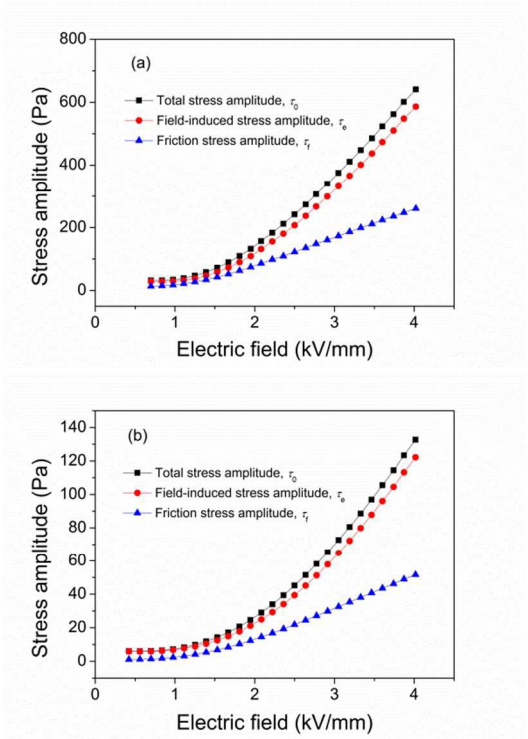

Figure 12. Dependence of the total shear stress amplitude, the field-induced stress amplitude, and the friction stress amplitude on electric field

Figure 13 shows the dependence of the friction stress amplitude and the contribution of friction on electric field. As the electric field increases, the friction stress amplitude of the two ER fluids increases, which is gently at low field level, and fast at high field level. Nevertheless, the contribution of the friction stress to the total stress (C_f) is not a monotonic function of the electric field. Initially, C_f increases with increasing electric field, while it decreases when the field exceeds a critical value. For both of the two ER fluids, their critical electric fields agree with the fields that the friction stress dramatically rises with increasing field. It is probably because the structures formed by the particles transit from chains to columns at the critical fields. It indicates for chain-like structures, the friction stress increase faster than the field-

induced shear stress as the electric field increases. In contrast, when column-like structures are formed at the critical fields, the field-induced shear stress rises faster than the friction stress. It also can be observed from Fig.13 that under the same electric field, the contribution of friction of C-ERF is higher than the S-ERF. The rough surface of the chrysanthemum-like particles may be responsible for this phenomenon.

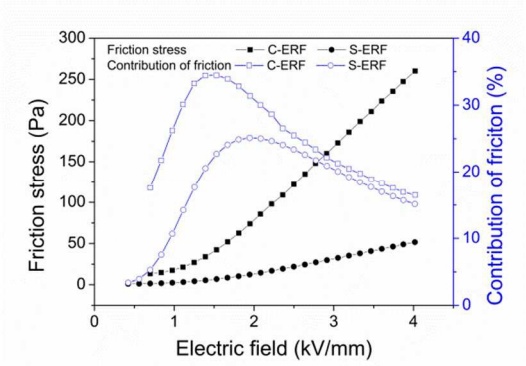

Figure 13. Dependence of the friction stress amplitude and the contribution of friction on electric field

5. Conclusions

Chrysanthemum-like particles-based ER suspension presents more significant ER performance than the ER fluid prepared with spherical particles. The enhancement of friction force caused by their rougher surface is an important reason for the improvement of ER properties. For both of the two ER fluids, the contribution of friction to ER activity increases with increasing electric field at low field levels, and decreases at high field levels. At the same electric field, the contribution of friction to ER effect in the chrysanthemum-like particles-based ER suspension is higher than that in the spherical particles-based one.

Acknowledgements

This work was supported by the National Natural Science Foundation of China under the grant number of 51478088 and the International Scientific & Technological Cooperation Program of China under the grant number of 2014DFA70950.

Notes and references

1 T. C. Halsey, *Science*, 1992, 258, 761
2 J. Rabinow, *AIEE Trans,* 1948, 67, 1308
3 J. Vicente, D. J. Klingenberg and R. Hidalgo-Alvarez, *Soft Matter,* 2011, 7, 3701
4 K. Q. Lu, R. Shen, X. Z. Wang, G. Sun and W. J. Wen, *International Journal of Modern Physics B*, 2005, 19, 1065
5 X. H. Liu, J. J. Guo, Y. C. Cheng, G. J. Xu, Y. Li and P Cui, *Rheol Acta*, 2010, 49, 837
6 Y. P. Qiao, J. B. Yin and X. P. Zhao, *Smart Materials and Structures*, 2007, 16, 332
7 L. M. Wang, X. Q. Gong and W. J. Wen, *Top Curr Chem*, 2011, 304, 91
8 K. Yoshida, K. Kamiyama, J. W. Kim and S. Yokota, *Sensors and Actuators*, 2012, A175, 101
9 B. Weinberg, A. Khanicheh, M. Sivak, O. Unluhisarcikli, G. Morel, J. Shannon, J. Kelliher, M. Sabadosa, G. Bonmassar, B. Patritti, P. Bonato and C. Mavroidis, *Third Joint Eurohaptics Conference and Symposium on Haptic Interfaces for Virtual Environment and Teleoperator Systems*, 2009, 529
10 J. Nikitczuk, B. Weinberg, P. K. Canavan and C. Mavroidis, *IEEE/ASME Transactions on Menhatronics,* 2010, 15, 952
11 W. M. Winslow, *Journal of Applied Physics*, 1949, 20, 1137
12 L. C. Davis, *J. Appl. Phys*, 1992, 74, 1334
13 H. J. Choi, M. S. Cho, J. W. Kim, C. A. Kim and M. S. Jhon, *Appl. Phys. Lett*, 2001, 78, 3806
14 J. E. Martin, J. Odinek, T. C. Halsey and R. Kamien, *Phys. Rev. E*, 1998, 57, 756
15 W. J. Wen, X. X. Huang, S. H. Yang, K. Q. Lu and P. Sheng, *Nature Materials*, 2003, 2, 727
16 R. Shen, X. Z. Wang, Y, Lu, D, Wang, G Sun, Z. X. Cao and K. Q. Lu, *Advanced materials*, 2009, 21, 1
17 X. Huang, W. J. Wen, S. H. Yang and P. Shen, *Solid State Communications*, 2006, 139, 581
18 C. G. Niu, X. F. Dong, H. Zhao and M. Qi, *Smart Materials and Structures*, 2014, 23, 075018
19 W. Bao, J. Zheng and X. F. Wu, *Journal of Physics*, 2012, 22, 1
20 A. Krzton-Maziopa, M. Gorkier and J. Plocharski, *Polymers for Advanced Technologies*, 2012, 23, 702
21 J. H. Wu, F. H. Liu, J. J. Guo, P. Cui, G. J. Xu and Y. C. Cheng, *Colloids and Surfaces A: Physicochemical and Engineering Aspects*, 2012, 410, 136
22 J. B. Yin, X. X. Wang, R.T. Chang and X. P. Zhao, *Soft Matter*, 2012, 8, 294
23 F. H. Liu, G. J. Xu, J. H. Wu, Y. C. Cheng, J. J. Guo and P. Cui, *Smart Materials and Structures*, 2009, 18, 125015
24 J. B. Yin, X. Xia, L. Q. Xiang and X. P. Zhao, *Smart Materials and Structures*, 2011, 20, 015002
25 W. J. Wen, X. X. Huang and P. Shen, *Soft Matter,* 2008, 4, 200
26 K. Q. Lu, R. Shen, X. Z. Wang, G. Sun, W. J. Wen and J. X. Liu, *Chinese Physics*, 2006, 11, 2476
27 P. Tan, W. J. Tian, X. F. Wu, J. Y. Huang, L. W. Zhou and J. P. Huang, *J. Phys. Chem. B*, 2009, 113, 9092
28 B. X. Wang and X. P. Zhao, *Advanced Functional Materials*, 2005, 15, 1815
29 Z. B. Wang, X. F. Song, B. X. Wang, X. L. Tian, C. C. Hao and K. Z. Chen, *Chemical Engineering Journal*, 2014, 256, 268
30 S. O. Carlos, J. B. He and H. M. Jaeger, *Soft Matter*, 2011, 7, 8023
31 J. L. Jiang, Y. D. Liu, L. Shan, X. J. Zhang, Y. G. Meng, H. J. Choi and Y. Tian, *Smart Mater. Struct.*, 2014, 23, 015003
32 Y. Tian, M. L. Zhang, J. L. Jiang, N. Pesika, H. B. Zeng, J. Israelachvili, Y. G. Meng and S. Z. Wen, *Physical Review E*, 2011, 83, 011401
33 J. L. Jiang, Y. Tian and Y. G. Meng, *Langmuir*, 2011, 27, 5814
34 W. H. Li and X. Z. Zhang, *Korea-Australia Rheology Journal ,* 2008, 20, 45
35 G. H. Tian, Y. J. Chen, W. Zhou, K. Pan, C. G. Tian, X. R. Huang and H. G. Fu, *CrystEngComm*, 2011, 13, 2994